3-D numerical model of the flexural isostatic response to extension induced by crustal scale listric normal faulting

Juan García Abdeslem
CICESE, División de Ciencias de la Tierra, Ensenada, B. C., México

RESUMEN

Se modela la respuesta flexural isostática de la litósfera, inducida por fallamiento lístrico normal, suponiendo que la región frágil de la corteza superior se extiende por cizalla simple, y que la región dúctil de la corteza inferior y manto superior se extienden por cizalla pura. A partir de la solución de la ecuación diferencial parcial que describe el estado de equilibrio, bajo la acción de las diversas cargas aplicadas, se obtienen expresiones analíticas simples para calcular la respuesta flexural isostática debida a fallamiento lístrico normal de escala cortical en un escenario 3-D. La aplicación de dichas expresiones se ilustra con un ejemplo donde se utiliza una falla lístrica normal y curvilínea definida analíticamente.

PALABRAS CLAVE: Isostasia, extensión cortical, fallamiento lístrico normal.

ABSTRACT

The flexural isostatic response of the lithosphere, induced by listric normal faulting, is modeled by assuming that simple-shear extension takes place in the brittle upper crust while the lower crust and upper mantle extend in pure shear. The partial differential equation describing the equilibrium state under the action of applied loads provides simple analytical expressions for computing the flexural isostatic response 3-D. An example using an analytically defined curvilinear normal fault is provided.

KEY WORDS: Isostasy, crustal extension, listric normal faulting.

INTRODUCTION

Isostasy is a process by which the Earth's surface elevation is adjusted in response to changes in mass density at depth or a redistribution of mass on its surface. The weight of surface loads is balanced by mass density anomalies in such a way that at some uniform depth the pressure is everywhere constant, in a state of hydrostatic equilibrium. Under ideal conditions all crustal columns exert equal pressure at this depth, and a column extending above sea level has a mass equal to the compensation mass at depth.

There are two main types of models of isostatic compensation, local and regional. In local models the compensating mass density is determined only by the topographic load above it, and compensation occurs by thickening a crust of constant mass density (Airy, 1885) or by lateral changes in crustal mass density (Pratt, 1885). Thus, any topographic load must give rise to vertical crustal movements. The lithosphere has zero strength and will creep or fail in response to any stress.

In regional compensation the lithosphere is assumed to behave as a composite layered body, where the upper crust behaves as an elastic plate while the lower crust and upper mantle behave as a fluid. The compensating mass density is distributed laterally on a regional basis (Banks *et al*., 1977;

Forsyth, 1985). In the regional flexural model, the response of the plate is characterized either by the flexural rigidity or by its effective elastic thickness. The Airy model corresponds to a regional compensation model of zero flexural rigidity.

The aim of this work is to examine the three-dimensional (3-D) flexural isostatic response of the lithosphere to extension induced by crustal scale listric normal faulting. This is relevant, in order to understand the geometry of sedimentary basins and crustal structure associated with rifting in the continental lithosphere. The upper crust is treated as a thin elastic plate overlying a fluid lower crust and mantle, assuming that the crust is mechanically decoupled from the mantle. Following Kuznir and Egan (1990), extension in the brittle upper crust occurs by simple-shear faulting, while pure-shear ductile deformation occurs in the lower crust and mantle lithosphere.

The response of the lithosphere is found by solving the partial differential equation that describes the equilibrium condition of a thin elastic plate (Banks *et al*., 1977; Turcotte and Schubert, 1982; Kuznir and Egan 1990; Egan, 1991). The solution is carried out numerically, in the wavenumber domain, using a discrete 2-D Fourier transform algorithm (Press *et al*., 1986).

I first describe the partial differential equation for the equilibrium condition of a thin elastic plate under the action of a distributed 3-D load. That is followed by the method used to construct the listric normal fault and basin geometries. Next, considering a final time frame in the extension process, the partial differential equation is adapted to compute the flexural isostatic response induced by crustal thinning, the response to pure-shear extension in the lower crust and mantle lithosphere, and the response to the load due to sediments infilling the basin.

FLEXURAL DEFLECTION OF A THIN PLATE

The flexural isostatic response of the lithosphere w caused by a distributed 3-D load can be modeled assuming that the crust behaves as a continuous and homogeneous thin elastic plate, which is in equilibrium under the action of all of the applied loads. Assuming that no horizontal forces are acting on the plate, the equilibrium equation (Turcotte and Schubert, 1982) is given by

$$D \cdot \nabla^4 w(x,y) + (\rho_m - \rho_l)gw(x,y) = p(x,y) , \quad (1)$$

where ∇^4 is the biharmonic differential operator, $D = ET^3/12(1-v^2)$ is the flexural rigidity of the elastic plate which determines the wavelength and amplitude of the deflection, E is Young's modulus, v is Poisson's ratio, T represents the effective elastic thickness of the plate, $p(x,y)$ is the net force per unit area exerted by the applied load, g is the gravitational acceleration, and ρ_m and ρ_l are the mass densities of the mantle and the load material, respectively.

The solution of (1) is accomplished in the wavenumber domain via the 2-D Fourier transform, and once the solution is achieved, its representation in the spatial domain is obtained via the 2-D inverse Fourier transform. The Fourier transform pair definition used in this work is given by

$$\Im[h(x,y)] = h(k_x, k_y),$$
$$= \int_{-\infty}^{\infty} \int_{-\infty}^{\infty} h(x,y) exp\left[-i2\pi(k_x x + k_y y)\right] \, dxdy \quad (2)$$

and

$$\Im^{-1}[h(k_x, k_y)] = h(x,y)$$
$$= \int_{-\infty}^{\infty} \int_{-\infty}^{\infty} h(k_x, k_y) exp\left[i2\pi(k_x x + k_y y)\right] dk_x dk_y \quad (3)$$

where k_x and k_y are wave numbers in the x- and y-directions.

THE LISTRIC NORMAL FAULT CONSTRUCTION

Normal faults are typically steeply dipping, usually in the range of 55° to 70°, but their dips can be even greater, approaching 90° in some near-surface faulting. However, some normal faults dip substantially less than 50°, even as low as a few degrees in the extreme. Normal faults that gradually flatten with depth are called listric normal faults.

Suppe (1985) pointed out several reasons for this large variation in dip of normal faults: Many normal faults pass downward into a relative flat stratigraphic décollement controlled by ductile lithological units of shale or salt, along which the hanging-wall fault block slides; More-deep-seated normal faults associated with crustal extension may flatten either abruptly or gradually into the ductile lower crust or upper mantle.

Listric normal faults flatten out at depth on a surface known as a detachment surface. According to Wernicke (1985), detachment surfaces act as relays that partition extension in the upper and lower lithosphere.

Following Egan (1991), the listric fault geometry F is defined here as

$$F(x,y) = Z_d\left[1 - exp\left(-f_0(x,y)/Z_d\right)\right], \quad (4)$$

where Z_d is the depth at which the fault detaches, and f_0 denotes the locations of points where the fault outcrops. The crustal thinning S produced by extension along this fault is

$$S(x,y) = F(x,y) - Z_d\left[1 - exp\left(-(f_0(x,y) - e(y))/Z_d\right)\right], \quad (5)$$

where x and y represent coordinates along the east and west directions, and e denotes the location of the maximum amount of extension, in the direction of tectonic transport, which is assumed here to be along the x-direction.

Equations (2) and (3) were used to outline a cross section containing a listric normal fault that outcrops at $f_0 = 0$ and detaches at a depth $Z_d = 20$ km, at three stages, where the location of the maximum extension lies at 10, 20 and 30 km (Figure 1).
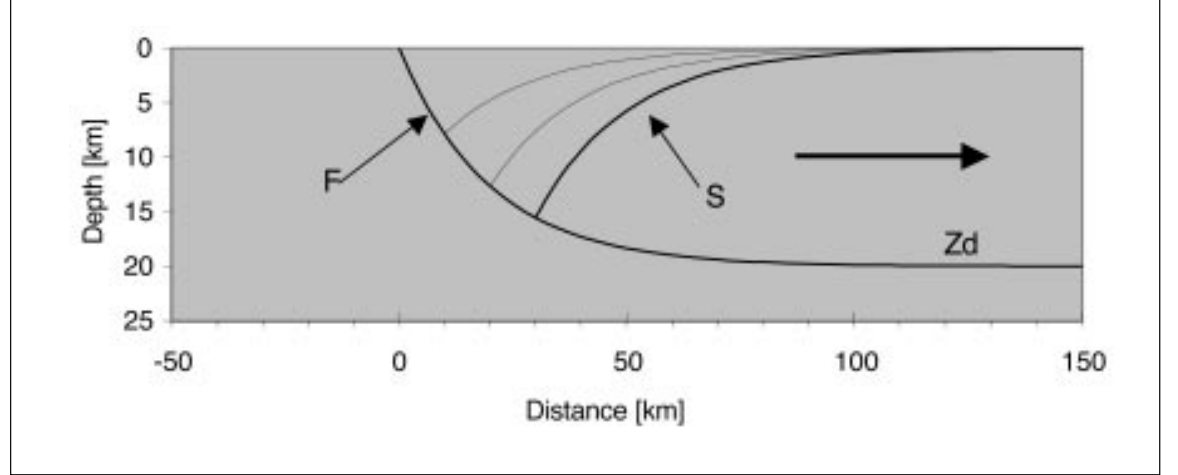
Fig. 1. A cross section of a listric normal fault, outcropping at the origin, is shown at 10, 20, and 30 km of maximum extension. The listric fault detaches at a depth of 20 km.

CRUSTAL THINNING BY LISTRIC NORMAL FAULTING AND FLEXURAL ISOSTATIC REBOUND

Consider the case of a 200 km long curvilinear listric normal fault that outcrops at discrete locations (x_i, y_i), where y_i takes regularly distributed values separated 2 km apart between $y = \pm 100$ km, and

$$x_i = 30 \sin\left[\frac{\pi}{2}(y_i - 100)/100\right]. \tag{6}$$

The listric normal fault detaches at a depth $Z_d = 20$ km, causing a maximum extension $e = 30$ km at $y_i = 0$, due to the hanging wall displacement along the eastward x-direction (Figure 2a).

The empty basin geometry S, created as the hanging wall is displaced in the tectonic transport direction (Figure 2a) can be treated as a negative load upon the crust, causing isostatic uplift. The differential equation at equilibrium state under the action of all applied loads is given by

$$D\nabla^4 w_s(x, y) + (\rho_m - \rho_a)g w_s(x, y) = -\rho_c\, g\, S(x, y), \tag{7}$$

where ρ_a and ρ_c are the mass densities of the air and crustal unloading material. Fourier transforming both sides of equation (7) yields

$$(2\pi k)^4 D w_s(k_x, k_y) + (\rho_m - \rho_a)g w_s(k_x, k_y) = -\rho_c\, S(k_x, k_y), \tag{8}$$

which can be written as

$$w_s(k_x, k_y) = -\left(\frac{\rho_c}{\rho_m - \rho_a}\right)\left(1 + \frac{(2\pi k)^4 D}{(\rho_m - \rho_a)g}\right)^{-1} S(k_x, k_y)\,, \tag{9}$$

where $k = \sqrt{k_x^2 + k_y^2}$, and inverse Fourier transforming this last result yields $w_s(x, y)$.

Considering an original crustal thickness $C_0 = 30$ km, the flexural isostatic rebound induced by crustal thinning due to listric normal faulting and the final configuration of the empty basin are shown in Figures 2b and 2c, respectively. A cross section of the 3-D geometry of the processes described above, along $y = 0$, is shown in Figure 3. The model parameters used in this and subsequent computations are listed on Table 1.

FLEXURAL ISOSTATIC RESPONSE TO DUCTILE EXTENSION IN THE LOWER CRUST AND UPPER MANTLE

In the ductile environment of the lower continental crust and upper mantle, extension is assumed to occur by a regionally distributed stretching or pure-shear ductile deformation (McKenzie, 1978; Egan, 1991). The amount of crustal thinning by pure-shear (P) is given by

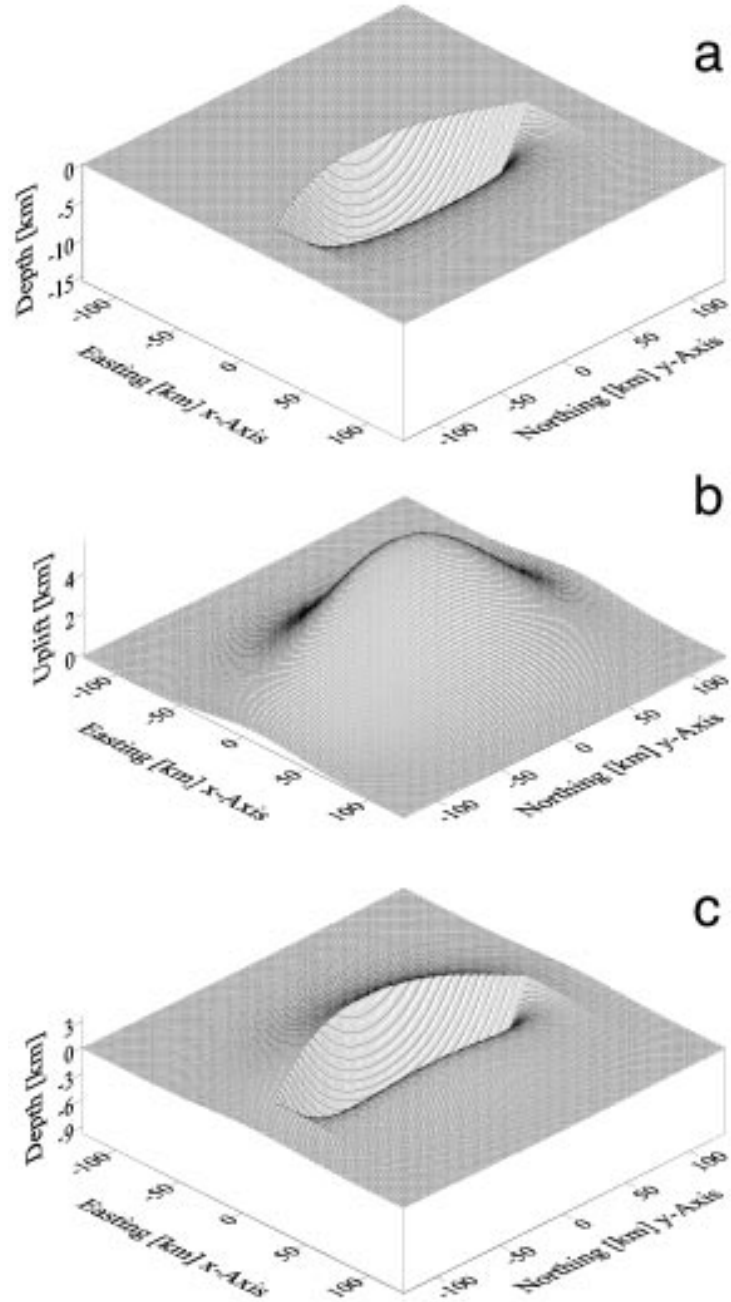$$P(x, y) = (C_0 - Z_d)[1 - 1/\beta(x, y)]\,, \tag{10}$$

43

Fig. 2. (a) 3-D view of a 200 km long listric normal fault is shown over a flat lying land at sea level. The fault detaches at a depth $Z_d = 20$ km, and the amount of extension varies from zero at the northern and southern extremes of the fault to a maximum of 30 km at $y = 0$, where the half-graben basin reaches a maximum depth of about 15.6 km, and it shallows eastward, approaching sea level in a distance of about 120 km. (b) The flexural isostatic response to 30 km of extension induces a regionally distributed uplift that varies accordingly with the amount of extension, reaching a maximum of about 5.7 km with respect to the base of the original crust. As a result of the flexural rebound the basin geometry is deformed (c). The basin shallows to a maximum depth of about 9.9 km below sea level, and the footwall is uplifted about 3.5 km above sea level.
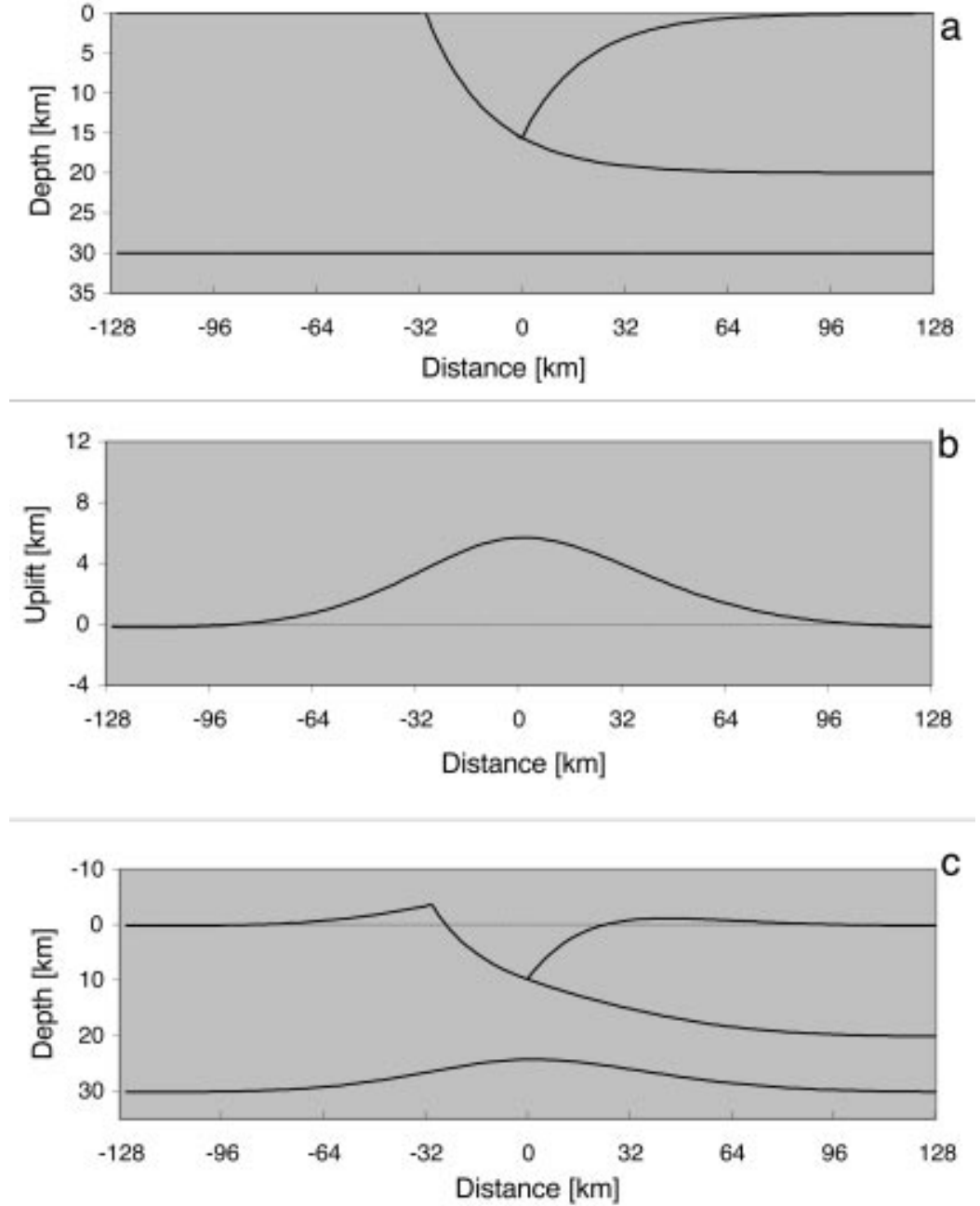
Fig. 3. Flexural isostatic response to 30 km of crustal extension induced by a listric normal fault (a) is shown in a cross section along $y = 0$. The uplift (b) is regionally distributed along some 290 km, causing (c) the Moho to shallow from an original depth $C_0 = 30$ km to about 24 km below sea level; both the foot wall and the hanging wall are uplifted, reaching maximum highs of 3.496 and 1.140 above sea level, respectively, and the maximum depth in the basin is 9.876 km below sea level.

where C_0 is the original crustal thickness, and β is the extension factor (McKenzie, 1978). Due to the ductile nature of the lower crust, the pure-shear extension is regionally distributed with respect of the localized faulting above, and β is

assigned a sinusoidal distribution such that

$$\beta(x,y) = \frac{\pi}{2}\left[e(y)/W - e(y)\right] sin(\pi x/W) + 1, \qquad (11)$$

45

Table 1

Assumed values for model parameters

Original crustal thickness	$C_0 = 30\ 000$ m
Young's modulus	$E = 1 \times 10^{11}$ Pa
Poison's ratio	$v = 0.25$
Effective elastic thickness	$T = 10\ 000$ m
Flexural rigidity	$D = 0.711 \times 10^{20}$ Nm
Density of air	$\rho_a = 0$ kg/m^3
Density of sediments	$\rho_s = 2400$
Density of crust	$\rho_c = 2670$
Density of mantle	$\rho_m = 3300$

where W is the width over which the pure-shear is distributed and e denotes the maximum extension along the y-axis. The resulting flexural subsidence (w_p) is calculated by solving the following differential equation:

$$D \cdot \nabla^4 w_p(x,y) + (\rho_m - \rho_a)gw_p(x,y) = (\rho_m - \rho_c)\, g\, P(x,y) \ .$$

(12)

Fourier transforming both sides of equation (12) yields the following result:

$$w_p(k_x,k_y) = \left(\frac{\rho_m - \rho_c}{\rho_m - \rho_a}\right)\left(1 + \frac{(2\pi k)^4 D}{(\rho_m - \rho_a)g}\right)^{-1} P(k_x,k_y),$$

(13)

and the inverse Fourier transform of this result yields $w_p(x,y)$.

In the current example, the listric normal fault is assumed to detach at a depth $Z_d = 20$ km, below which extension occurs by pure-shear. The amount of crustal thinning by pure-shear (P) varies between zero, coinciding with the basin's limits above, and some 2 km, up from the original crustal thickness, and it is symmetrically distributed along and across the basin above (Figure 4a). The flexural subsidence (w_p) induced by the mass unbalance is a smoother version of the former, with maximum amplitude less than 500 m. The crustal thinning and the flexural subsidence, induced by pure-shear in the lower crust are shown (Figure 5) in a cross section along $y = 0$.

FLEXURAL ISOSTATIC RESPONSE BY SEDIMENTS FILLING THE BASIN

The material infilling the created basin acts as a downward acting load upon the lithosphere inducing further subsidence, and the flexural isostatic subsidence (w_i) resulting from the basin fill is calculated from the solution of the following differential equation:

$$D \cdot \nabla^4 w_i(x,y) + (\rho_m - \rho_i)gw_i(x,y) = \rho_i\, g\, B(x,y),$$

(14)

where B defines the basin depth to be filled with material of mass density ρ_i. Fourier transforming both sides of equation (14) yields the following result:

$$w_i(k_x,k_y) = \left(\frac{\rho_i}{\rho_m - \rho_i}\right)\left(1 + \frac{(2\pi k)^4 D}{(\rho_m - \rho_i)g}\right)^{-1} B(k_x,k_y),$$

(15)

and the inverse Fourier transform of this last result yields $w_i(x,y)$.

After crustal thinning by listric normal faulting, flexural isostatic rebound, and ductile extension in the lower crust and upper mantle, the originally flat lying land is deformed to reach the geometry shown in Figure 6a. In the last stage the empty basin is filled with sediments of mass density ρ_i, which causes additional subsidence (Figure 6b) and the final geometry shown in Figure 6c. In Figure 7 this last stage results are shown in a cross section along $y = 0$.

CONCLUSION

The flexural isostatic response to crustal extension induced by crustal scale listric normal faulting is examined in a three-dimensional scenario. Assuming that no horizontal forces are acting upon it, the upper crust is treated as a continuous and homogeneous thin elastic plate, which is in equilibrium under the action of all of the applied loads.

Using a simple analytical description for the listric normal fault geometry, the flexural isostatic response of the lithosphere, caused by a distributed 3-D load, is modeled assuming that simple-shear extension takes place in the brittle upper crust, while the lower crust and upper mantle extend by pure-shear ductile deformation. The partial differential equation describing the equilibrium state, under the action of all of the applied loads, is solved in the
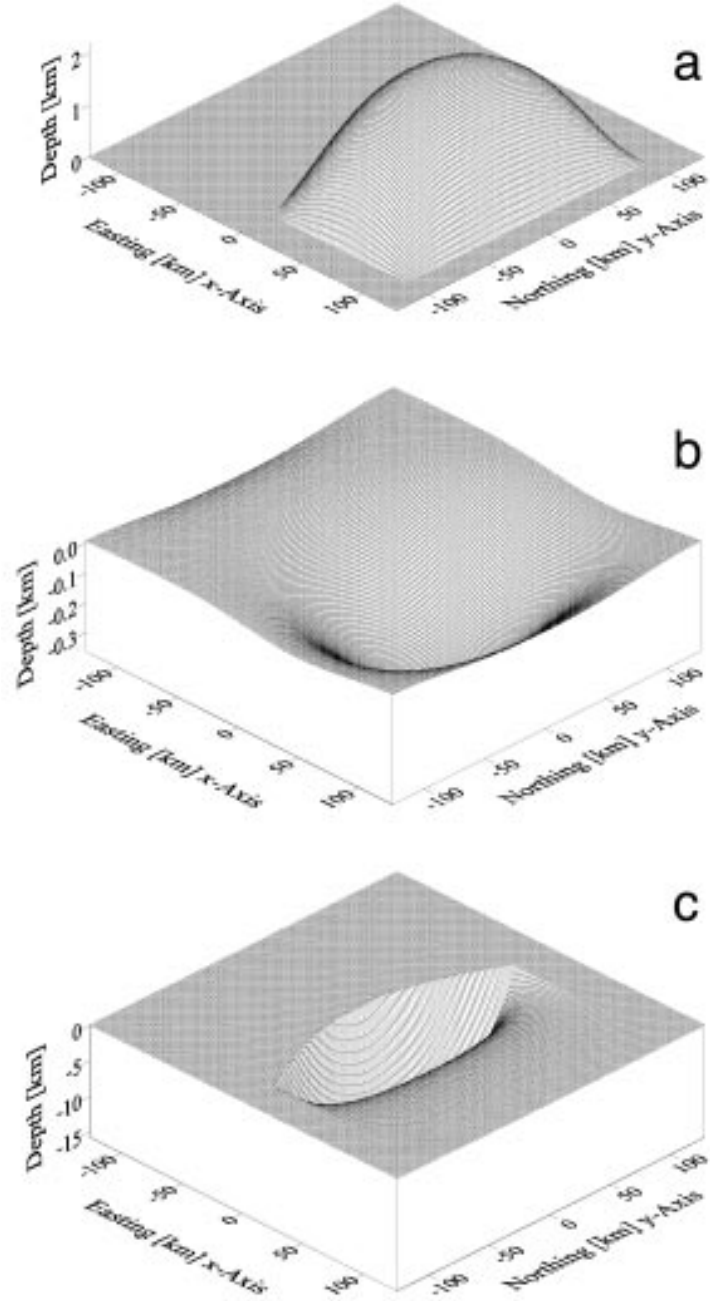
Fig. 4. The listric normal fault is assumed to detach at a depth $Z_d = 20$ km, below which extension occurs by pure-shear. The crustal thinning by pure-shear (a) is symmetrically distributed along and across the basin above. The flexural subsidence (b) induced by the mass unbalance is a smoother version of the former, and as a result the basin geometry is modified (c).

wavenumber domain, providing simple formulae to compute the flexural isostatic response to crustal extension induced by crustal scale listric normal faulting in a three-dimensional scenario. The formulae and methods reported here are illus-trated with one example using a curvilinear listric normal fault with variable amount of extension, where the partial differential equations are solved using a 2-D discrete Fou-rier transform algorithm.
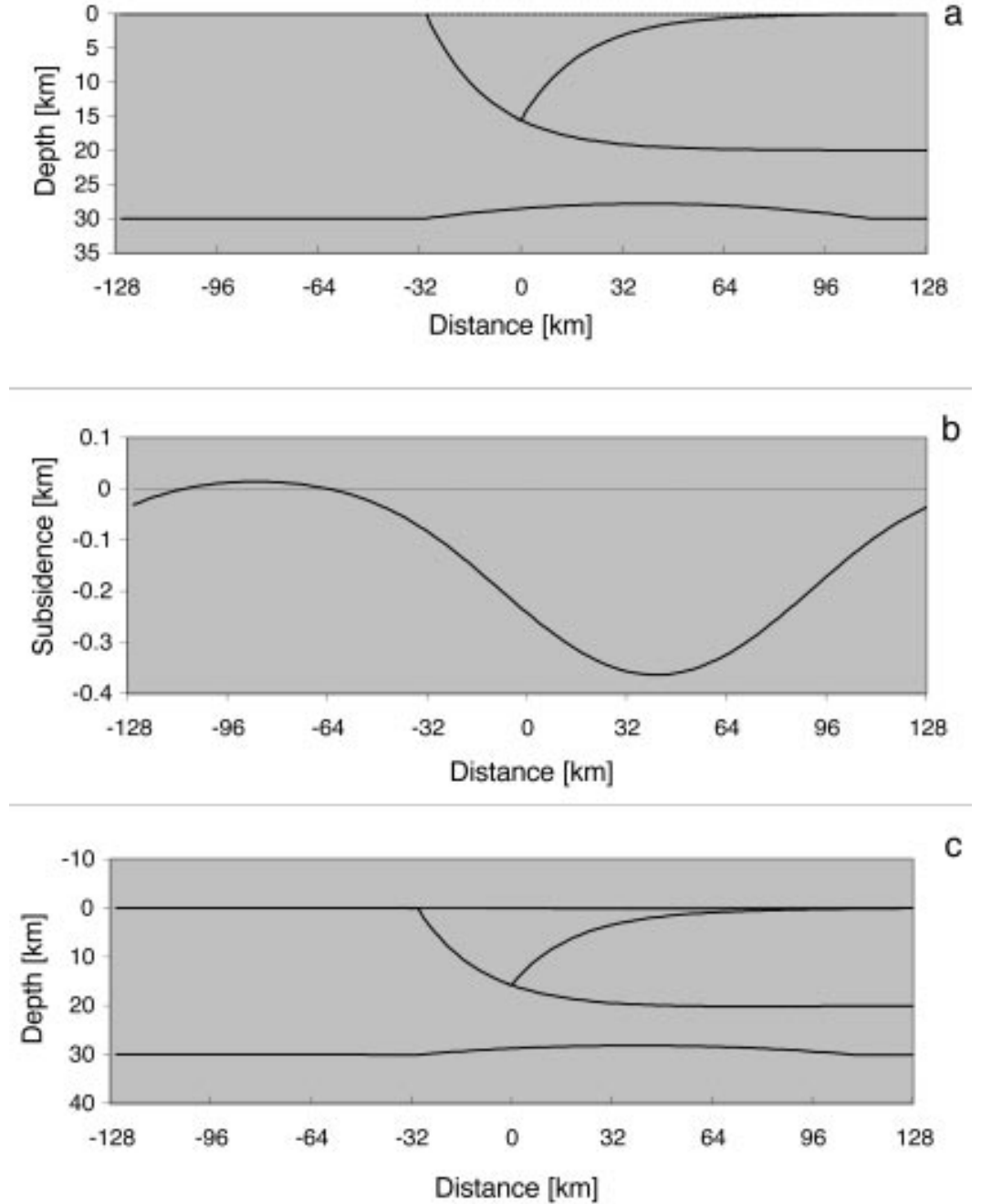
Fig. 5. Crustal thinning and flexural subsidence, induced by pure-shear in the lower crust and upper mantle, are shown in a cross section along $y = 0$. The crustal thinning by pure-shear (a) is symmetrically distributed along some 142 km, coinciding with the basin's limits above, its maximum reaches 27.857 km below sea level and it is located under the eastern basin's margin. The flexural subsidence (b) induced by the mass unbalance is a smoother version of the former, with maximum amplitude of some 363 m, which furthers deforms the basin geometry (c).
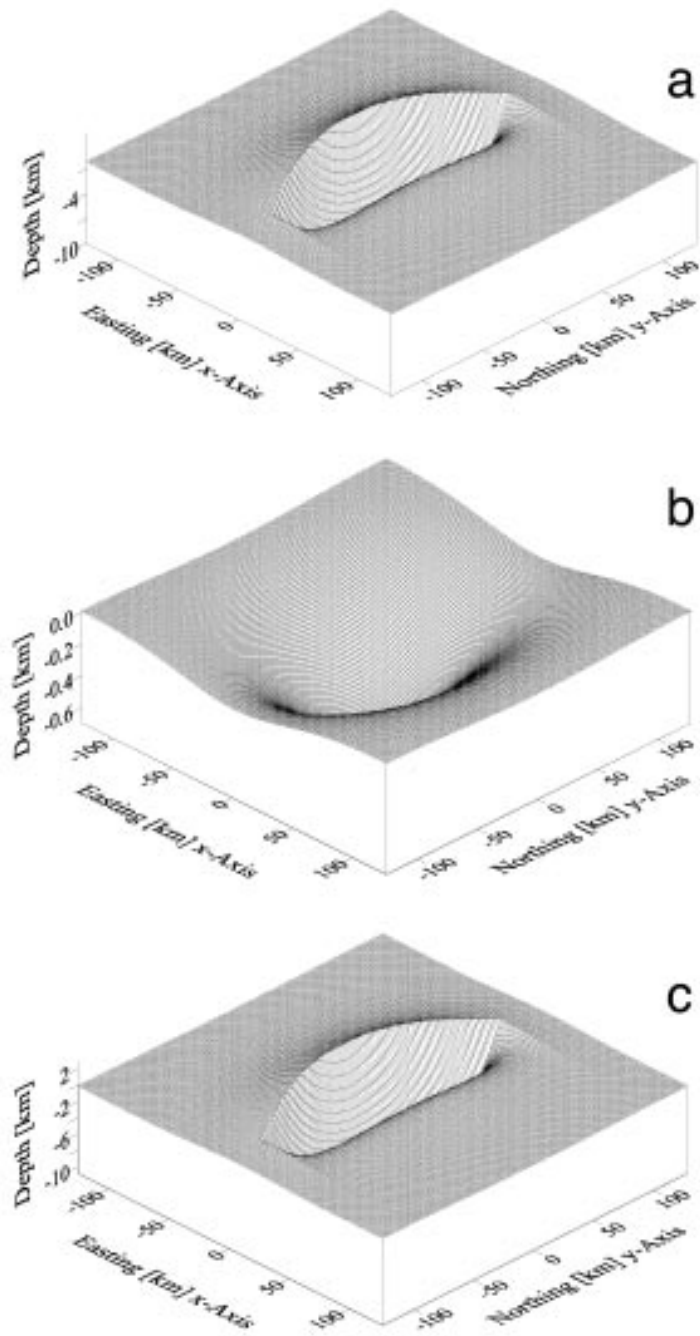
Fig. 6. After crustal thinning by listric normal faulting, flexural isostatic rebound, and ductile extension in the lower crust and upper mantle, the originally flat lying land is shown in (a). Filling the basin with sediments of mass density ρ_i causes additional subsidence (b), and the final geometry shown in (c).
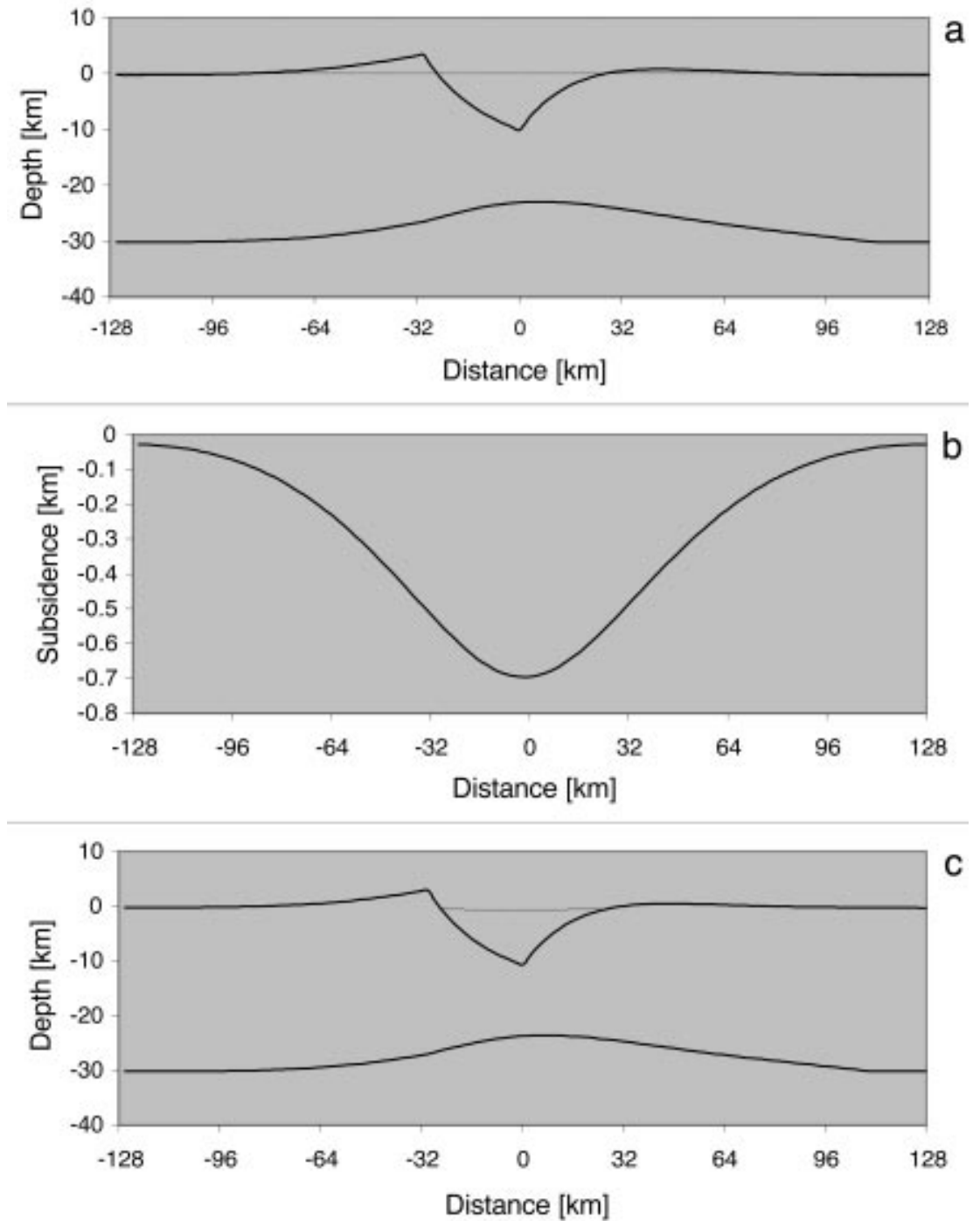
Fig. 7. After crustal thinning by listric normal faulting, flexural isostatic rebound, and ductile extension in the lower crust and upper mantle, the originally flat lying land is shown (a) in a cross section along $y = 0$. Filling the basin with sediments of mass density ρ_i causes additional subsidence (b) that is regionally distributed with a maximum deflection of about 700 m. In the final geometry (c) the maximum footwall uplift is 2.87 km above sea level, while the hanging wall is only about 400 m ASL and the maximum basin depth is 10.8 km BSL. The final mantle uplift is at about 23.7 km below sea level.

BIBLIOGRAPHY

AIRY, G. B., 1855. On the computation of the effect of the attraction of mountain-masses as disturbing the apparent astronomical latitude of stations in geodetic surveys, Philos. *Trans. R. Soc. London, 145,* 101-104.

BANKS, R. J., R. L. PARKER and S. P. HUESTIS, 1977. Isostatic compensation on a continental scale: Local versus regional mechanisms. *Geophys. J. R. Astron. Soc., 51,* 431-452.

EGAN, S. S., 1992. The flexural isostatic response of the lithosphere to extensional tectonics. *Tectonophys., 202,* 291-308.

FORSYTH, D. W., 1985. Subsurface loading and estimates of the flexural rigidity of continental lithosphere. *J. Geophys. Res., 90,* 12,623-12,632.

KUZNIR, N. J. and S. S. EGAN, 1990. Simple-shear and pure-shear models of extensional sedimentary basin formation: Application to Jean d'Arc basin, Grand Banks of Newfoundland. *In:* Tankard, A. J., and Blackwill, H. R., eds. Extensional Tectonics of the North Atlantic Margins, AAPG Memoir 46, pp. 305-322.

McKENZIE, D. P., 1978. Some remarks on the development of sedimentary basins. *Earth Planet. Sci. Lett., 40,* 25-32.

PRATT, J. H., 1855. On the attraction of the Himalaya Mountains and of the elevated regions beyond them, upon the plumb line in India, *Philos. Trans. R. Soc. London, 145,* 53-100.

PRESS, W. H., B. P. FLANNERY, S. A. TEUKOLSKY and W. T. VETTERLING, 1986. Numerical Recipes: The art of scientific computing, Cambridge University Press.

SUPPE, J., 1985. Principles of Structural Geology, Prentice-Hall, Englewood Cliffs, N. J., 537 pp.

TURCOTTE, D. L. and G. SHUBERT, 1982. Geodynamics: Application of continuum Physics to Geological Problems, Wiley, New York, N.Y., 450 pp.

WERNICKE, B., 1985. Uniform sense normal simple shear of the continental lithosphere. *Can. J. Earth Sci., 22,* 108-125.

———————

Juan García Abdeslem

CICESE, División de Ciencias de la Tierra
Carretera Tijuana-Ensenada, km 107,
Ensenada, B. C., México
Email: jgarcia@cicese.mx